

IN DISGUISE OR OUT OF REACH: FIRST CLUES ABOUT IN-SITU AND ACCRETED STARS IN THE STELLAR HALO OF THE MILKY WAY FROM GAIA DR2

M. HAYWOOD AND P. DI MATTEO

GEPI, Observatoire de Paris, PSL Research University, CNRS, Sorbonne Paris Cité, 5 place Jules Janssen, 92190 Meudon, France

M. D. LEHNERT

Sorbonne Université, CNRS UMR7095, Institut d'Astrophysique de Paris, 98 bis bd Arago, 75014 Paris, France

O. SNAITH

School of Physics, Korea Institute for Advanced Study, 85 Hoegiro, Dongdaemun-gu, Seoul 02455, Republic of Korea

S. KHOPERSKOV AND A. GÓMEZ

GEPI, Observatoire de Paris, PSL Research University, CNRS, Sorbonne Paris Cité, 5 place Jules Janssen, 92190 Meudon, France

Draft version December 14, 2024

ABSTRACT

We investigate the nature of the double color-magnitude sequence observed in the Gaia DR2 HR diagram of stars with high transverse velocities. The stars in the reddest-color sequence are likely dominated by the dynamically-hot tail of the thick disk population. Information from Nissen & Schuster (2010) for some of the stars along the color-magnitude sequence suggests that stars in the blue-color sequence have elemental abundance patterns that can be explained by this population having a relatively low star-formation efficiency during its formation. A low star formation efficiency provides an evolutionary connection between stars with high-alpha abundances and low metallicities, $[\text{Fe}/\text{H}] < -1.1$ dex, and stars with low-alpha abundances and higher metallicities. In dynamical and orbital spaces, such as the “Toomre diagram”, the two sequences show a significant overlap, but with a tendency for stars on the blue-color sequence to dominate regions with no or retrograde rotation and high total orbital energy. In the plane defined by the maximal vertical excursion of the orbits, z_{max} , versus their apocenters, $R_{2D\text{max}}$, stars of both sequences redistribute into discrete wedges and we observe a dearth of stars with intermediate values of z_{max} . We conclude that stars which are typically assigned to the halo in the solar vicinity, i.e., those having either slightly prograde or retrograde orbits, are actually both accreted stars lying along the blue sequence in the HR diagram, and the low velocity tail of the old Galactic disk, possibly dynamically heated by past accretion events. Our results imply that a halo population that formed *in situ* and was responsible for the early chemical enrichment prior to the formation of the thick disk is yet to be robustly identified.

Keywords: Galaxy: evolution — Galaxy: kinematics and dynamics — Galaxy: halo

1. INTRODUCTION

Over the past three decades, a consensus has developed that the stellar halo of the Milky Way is composed of two populations of stars – those that were born in other galaxies and accreted and those that were born *in situ* during the early evolution of the Milky Way (e.g. Searle & Zinn 1978; Sommer-Larsen & Zhen 1990; Carollo et al. 2008). Although these two components have remained challenging to characterize, we now have a widely-accepted picture whereby the *in situ* halo population is older, more metal-rich, dominates the stellar density within ~ 15 kpc of the Galactic center, and has a slightly enhanced mean rotation rate compared to the accreted halo population (e.g., Carollo et al. 2008). While a considerable amount of effort is currently being expended investigating stellar streams that are expected to fill the outer stellar halo, the inner halo population is still lacking a proper characterization, and its evolutionary connection with the thick disk is essentially unknown.

The second data release (Gaia Collaboration et al. 2018a) of the European Space Agency’s Gaia mission (Gaia Collaboration et al. 2016) provides superb astrometric parameters, radial velocities and photometry for a large number of stars. First results have already detected a number of streams and kinematic groups (Malhan et al. 2018; Koppelman et al. 2018). Inspection of the Gaia HR diagram (hereafter HRD) of stars with high total or tangential velocities has shown two parallel color sequences (Gaia Collaboration et al. 2018b), which were attributed to stars in the thick disk and stellar halo. Here, we concentrate on understanding the origin of these two sequences and in particular the nature of the blue-color sequence. The next section describes our selection from the Gaia archive, Section 3 analyzes the sample of stars from Nissen & Schuster (2010) specifically with respect to where stars in this sample lie in these two sequences and thus bringing insights into the characteristics of the blue-color sequence. In Section 4, we present their main kinematic and orbital properties and we discuss our results and summarize our main conclusions in Section 5.

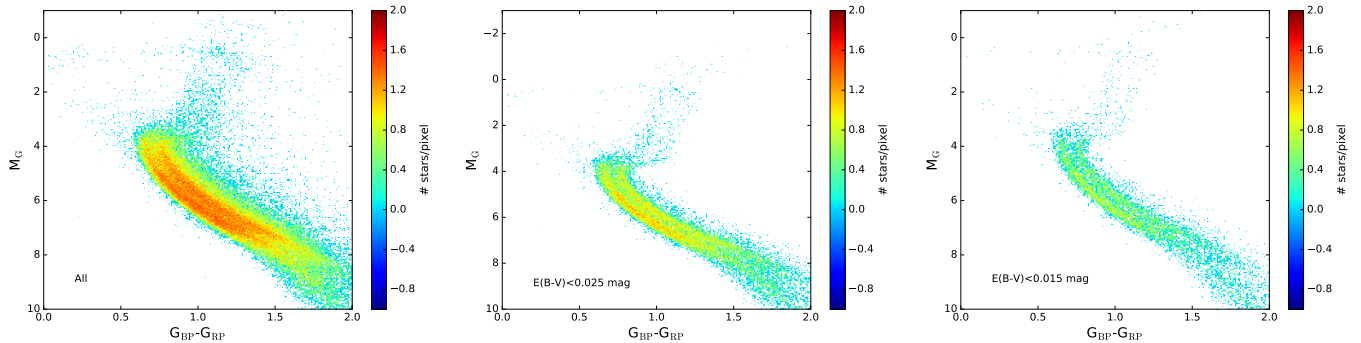


Figure 1. HRD of stars selected in Section 2, with different tolerances in the reddening. The two, blue- and red-color sequences, are well separated.

2. GAIA DR2 DATA

We select stars in the Gaia archive having a tangential velocity greater than 200 km.s^{-1} , parallax errors $\sigma_\pi/\pi < 0.1$, $\pi > 1$ mas, $G < 17$, and the filters described in Gaia Collaboration et al. (2018b). This brings us 77107 stars displayed in the HRD of Fig. 1 (left panel). This figure shows that the HRD separates in two sequences, as in Gaia Collaboration et al. (2018b), and which we designate below as the blue and the red sequence (BS and RS, respectively).

In order to clean the HRD, we select stars with various levels of tolerance on the interstellar reddening. We adopt the interstellar reddening estimates from the map of Lallement et al. (2018), which is well adapted for stars nearer than 1 kpc. Fig. 1 (middle and right panels) shows the HRD obtained by selecting stars that have levels of reddening below 0.025 and 0.015 mag, providing respectively 28210 and 12620 objects.

3. CLUES FROM THE SAMPLE OF NISSEN & SCHUSTER (2010)

The sample of Nissen & Schuster (2010) (hereafter NS) in different metallicity intervals is overplotted to the Gaia HRD in Fig. 2. This figure shows that the red and blue sequences are dominated by metal-rich ($[\text{Fe}/\text{H}] > -0.8$ dex) and metal-poor ($[\text{Fe}/\text{H}] < -1.1$ dex) stars (as already anticipated in Gaia Collaboration et al. 2018b). Note that the spread in metallicity in each sequence is significant, ~ 0.6 dex. A cross-match between 226 stars with metallicity measurements from APOGEE and our Gaia sample, shows that there is a marked dip in the metallicity distribution of stars at $[\text{Fe}/\text{H}] \sim -1.0$ dex (Gaia Collaboration et al. 2018b). This dip is also noticeable in the data of NS (their Fig. 1). The middle plot of Fig. 2 shows that stars with $-1.1 < [\text{Fe}/\text{H}] < -0.8$ dex, which brackets the dip in metallicity, fall between the two sequences of the HRD. This implies that the clear separation between the two sequences is the conspicuous consequence of the dip in the metallicity distribution function (MDF). Moreover, the middle plot shows that, at similar metallicities, low- α stars tend to be bluer than high- α ones, suggesting that they must be slightly younger, supporting similar results from Schuster et al. (2012). On the contrary, the bottom panel of Fig. 2 shows that low and high- α stars with $[\text{Fe}/\text{H}] < -1.1$ dex from the NS sample can both be found along the BS stars. This is surprising, because – given the tightness of the blue-color sequence – if the low and high alpha stars at $[\text{Fe}/\text{H}] <$

1.1 dex were belonging to two different chemical evolution sequences – as they do at $-1.1 < [\text{Fe}/\text{H}] < -0.8$ dex – we would expect a difference in age that would reflect in the HRD, as is seen for their more metal-rich counterparts (Fig. 2, middle plot). Is it thus possible that all the stars with $[\text{Fe}/\text{H}] < -1.1$ dex – both high or low α stars, because the distinction becomes less obvious below this metallicity – are the same population of stars, and are not causally related to the thick disk? Could they instead be causally related to the low- α sequence at higher metallicities, which is clearly distinct from the thick disk?

By analyzing the $[\text{Fe}/\text{H}]$ - $[\text{Mg}/\text{Fe}]$ distribution of APOGEE stars, Hayes et al. (2018) have shown that the separation between the high and low- α stars is not horizontal – it is not a separation in α -abundances – but that high- α stars at $[\text{Fe}/\text{H}] \lesssim -1.1$ dex and low- α stars at higher metallicities form a unique chemical sequence. The findings of Hayes et al. (2018) strongly support our suggestion. Fig 3 shows the $[\text{Fe}/\text{H}]$ - $[\alpha/\text{Fe}]$ distribution of the sample of Nissen & Schuster (2010), with the high-alpha, low metallicity stars shown as blue square. Indeed, these objects are all within the BS. It is therefore reasonable to suggest that the low-metallicity ($[\text{Fe}/\text{H}] < -1.1$ dex) stars of NS and the low- α sample at higher metallicity are forming a unique abundance sequence. The gap in the MDF at $[\text{Fe}/\text{H}] \sim -1$ dex could simply be a reflection of the transition between two populations of stars: a population whose origin needs to be determined (see below) at $[\text{Fe}/\text{H}] < -1$ dex, and the thick disk above this limit. Hayes et al. (2018) also mention that the transition between the two sequences in the $[\text{Fe}/\text{H}]$ - $[\alpha/\text{Fe}]$ plane is more pronounced at this metallicity (see also Bonaca et al. 2017).

4. KINEMATICS AND ORBITS

Of the sample of 28210 stars with $E(B-V) < 0.025$ mag, 1973 stars have full 3D velocity information in Gaia DR2. In all the following, we have assumed an in-plane distance of the Sun from the Galactic center $R_\odot = 8.34$ kpc following Reid et al (2014), a height of the Sun above the Galactic plane $z_\odot = 27$ pc (Chen et al 2001), a velocity for the Local Standard of Rest $V_{\text{LSR}} = 240 \text{ km.s}^{-1}$ (Reid et al 2014) and a peculiar velocity of the Sun with respect to the LSR $U_\odot = 11.1 \text{ km.s}^{-1}$, $V_\odot = 12.24 \text{ km.s}^{-1}$, $V_\odot = 7.25 \text{ km.s}^{-1}$, following Schonrich et al (2010).

The distributions of our stars in kinematic spaces is shown in Fig. 4, where we distinguish stars according to their lying on the blue or red sequences. We use the the

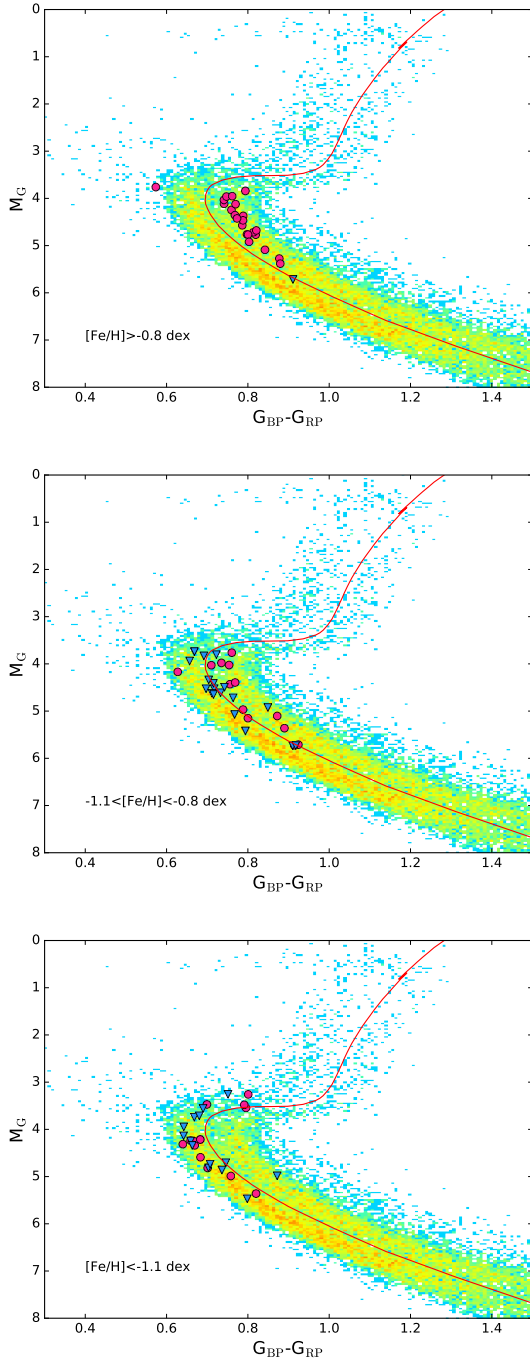


Figure 2. Overplotted on the Gaia HRD, stars from Nissen & Schuster (2010) with: $[\text{Fe}/\text{H}] > -0.8$ dex (*top panel*), $-1.1 < [\text{Fe}/\text{H}] < -0.8$ dex (*middle panel*), $[\text{Fe}/\text{H}] < -1.1$ dex (*bottom panel*). Thick disk and high- α halo stars from NS are represented with red circles, low- α halo stars from NS with blue triangles. The red line shows the isochrone from the PARSEC library used to separate the stars of the blue- and red-color sequences in the two sub-samples used in section 4.

isochrone in Fig. 2 to separate the two sequences. The two sequences overlap in the Toomre diagram, however the majority of stars on the RS, $\approx 75\%$, shows prograde rotation and lies in the region of the diagram that is compatible with the slow rotating tail of the thick disc (Fig. 4). The remaining fraction, 1/4 of red-color sequence stars, however, has retrograde orbits, lagging the

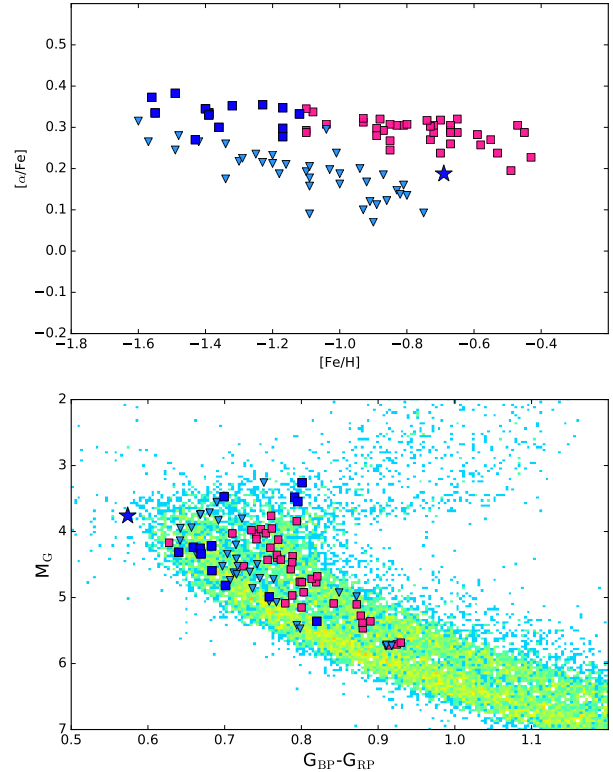


Figure 3. *Top:* the low- and high alpha stars from Nissen & Schuster (2010, triangles and squares). The high-alpha stars at $[\text{Fe}/\text{H}] < -1.2$ plotted as blue squares are assumed to be part of the same chemical sequence (Hayes et al. 2018). *Bottom:* the resulting classification is more consistent with the belonging to the two sequences in the HRD, see Fig.2. The star G81-02, originally classified as a 'halo' high-alpha star in Nissen & Schuster (2010), can also be classified as a low-alpha star (star symbol of both plots).

LSR by $\sim 400 \text{ km s}^{-1}$ or less. Except for 13 stars with very significant retrograde motions, $V < -500 \text{ km/s}$, that we will discuss in the following, stars on the BS are distributed over the same area as the RS stars in the Toomre diagram, but in different proportions. In particular, they dominate the extended vertical plume at null or retrograde rotation, with about 65% of BS stars lying within the region with $-350 \text{ km/s} \leq V \leq -200 \text{ km/s}$, while 26% have $V > -200 \text{ km/s}$ and the remaining fraction $V < -350 \text{ km/s}$. Remarkably, stars of the BS with prograde orbits clearly overlap with those of RS stars.

The same main structures visible in the Toomre diagram are found also in the $E - L_z$ plane (Fig. 4), where the energy E is the total energy of a star, defined as the sum of its kinetic and gravitational potential energies. We assume a Allen & Santillan (1991) Galactic mass model to estimate the latter. In this plane, we note that the RS stars around $L_z = 0$ are predominately on very bound orbits (i.e., low E). In the $L_z - L_{\text{perp}}$ plane, where

$L_{\text{perp}} = \sqrt{L_x^2 + L_y^2}$, there is significant overlap between the BS and RS within this space, except in two regions: (1) the region where the most extreme counter-rotating stars lie, which is composed of stars exclusively from the blue-color sequence; and (2) an over-dense region roughly centered at $(L_z, L_{\text{perp}}) \approx (1500, 2200) \text{ kpc}\cdot\text{km s}^{-1}$, which is very close to the region occupied by the Helmi stream ($(L_z, L_{\text{perp}}) \approx (1000, 2000) \text{ kpc}\cdot\text{km s}^{-1}$, see Helmi et al.

1999), which is also exclusively made of stars on the BS.

Finally, for all stars with full 3D velocity information, we have reconstructed their orbital parameters, by integrating their orbits over the last 6 Gyr, using three different Galaxy potentials: the axisymmetric potential of Allen & Santillan (1991) and the two axisymmetric potentials, including a thick disc component, in Pouliaxis et al (2017). In Fig 4, we show their distribution in the $z_{\max} - R_{2D,\max}$ plane, where z_{\max} is the maximum height that stars reach above or below the Galactic plane and, $R_{2D,\max}$, is the apocenter of their orbit projected on the Galactic plane. For clarity, we show in this plot only the orbital parameters that have been derived by integrating the orbits in the Allen & Santillan (1991) potential. Predominately, the stars on the RS have $R_{2D,\max}$ within 20 kpc of the Galactic center, while the orbits of stars on the BS can extend much further out than 20 kpc. A striking feature is that the stars in our sample are not homogeneously distributed in this plane, but define three distinct diagonal “wedges”, with z_{\max} increasing with $R_{2D,\max}$, indicating the presence of multiple and distinct flares¹.

Remarkably, one of these three patterns defines stars confined in a relatively thin and flattened distribution, with a lack of stars between $2 \leq z_{\max} \leq 4$ kpc. This lack of stars with z_{\max} in this range makes this region distinct from the rest of the sample. Ten of the thirteen stars with very significant retrograde motions, $V < -500$ km s⁻¹, are found in this thin flattened disc. Note that the presence of two groups of halo stars, a first with a flattened distribution and a second with more vertically extended orbits was already noted by Schuster et al. (2012, see their Fig. 8). We confirm and extend their findings with a significantly larger sample of stars.

5. DISCUSSION AND CONCLUSIONS

Our results provide new information about the possible origin of the stellar populations that dominate the two sequences in the HRD. If the metal-rich stars of Nissen & Schuster (2010) are representative of the red sequence, this sequence must be dominated by α -rich stars, with metallicities between -0.4 and -1 dex. We have also determined that the majority of RS stars are on prograde orbits. These are all characteristics typical of stars in the old thick disk (Haywood et al. 2013). An important result is that a non-negligible fraction of RS stars are on retrograde orbits. This can be at least partially attributed to an imperfect separation of stars of the BS and RS in the HRD – that is, part of the RS stars with very low or retrograde tangential velocities may be in fact BS stars which have been incorrectly assigned to the RS. However, an *in situ* stellar disk, dynamically heated by one or several satellite accretion events, will also have counter-rotating stars (see Jean-Baptiste et al. 2017). Hence, finding some non-rotating or counter-rotating stars among an *in situ* old disk population is not surprising. Although they have chemical characteristics typical of the thick disk, RS stars have the kinematics of halo stars (see also Bonaca et al. 2017; Posti et al. 2017).

¹ These three patterns are recovered also when we adopt Model I from Pouliaxis et al (2017) for the orbit integration, while in the case of Model II from Pouliaxis et al (2017), the distinction between the two higher- z wedges is less obvious, but still the one nearer to the Galactic plane is clearly distinct from the rest of the sample.

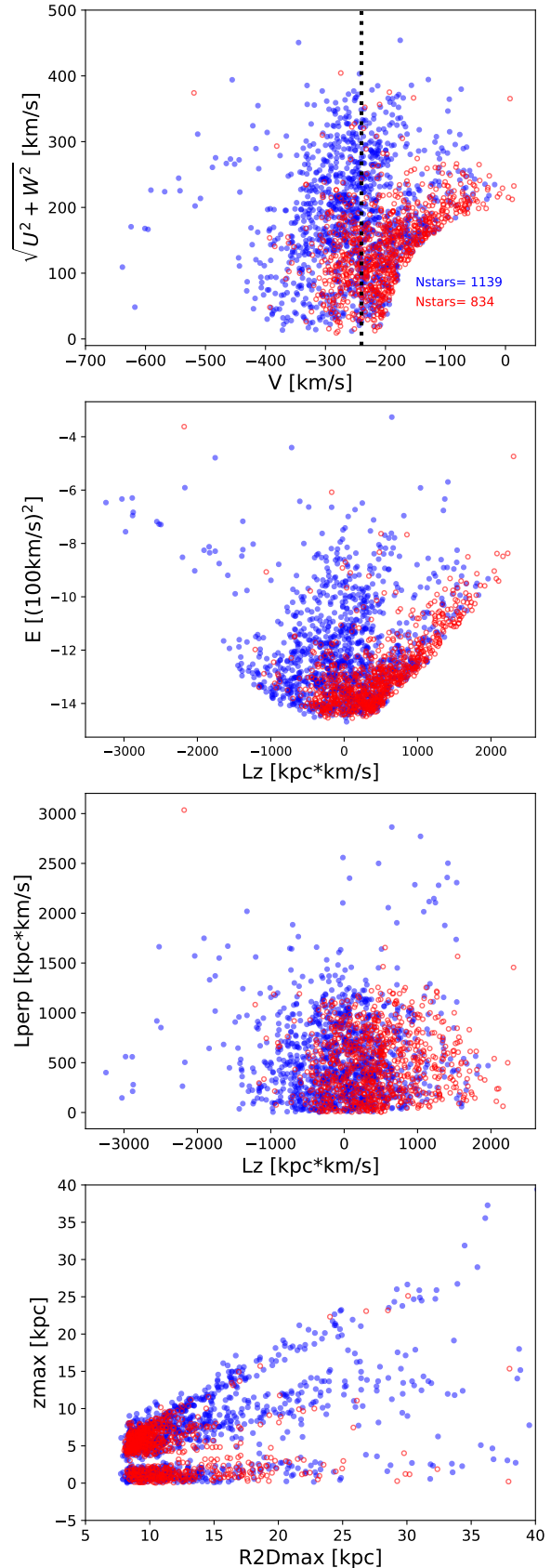


Figure 4. *From top to bottom:* Toomre diagram, $E - L_z$, $L_z - L_{\text{perp}}$ and $z_{\max} - R_{2D,\max}$ planes for all stars in our sample with full 3D velocities in Gaia DR2. The dashed line in the top plot indicates $V = -V_{\text{LSR}}$. In the bottom panel, only stars with $R_{2D,\max} \lesssim 40$ kpc have been plotted. In all panels, stars on the blue sequence are shown as filled blue dots, stars on the red sequence with empty red circles.

The most likely origin of the red-color sequence is thus related to the old Galactic disk, partially heated during some past accretion event(s).

Gaia Collaboration et al. (2018b) suggest that the blue-color sequence may be related to the in-situ halo. Low metallicity, $[\text{Fe}/\text{H}] < -1.1$ dex, high- α stars from Nissen & Schuster (2010) are indeed on the BS. However, our analysis shows that also low-metallicity, low- α stars are on this sequence (§ 3). Based on the fact that they belong to the same narrow sequence in the HRD and on the results of Hayes et al. (2018), we conjecture that the high- α stars with $[\text{Fe}/\text{H}] < -1.1$ dex could be causally connected to the higher metallicity, low- α stars forming a unique chemical evolution sequence. If these stars are on the same evolutionary sequence, they must have been formed in an environment characterized by a low star formation efficiency (i.e. long star formation time-scale), much lower than that of the thick disk. For this sequence, Supernovae-Ia must have started enriching the interstellar medium in Fe at lower metallicities compared to what is observed for thick disk stars of the Milky Way. The low- α stars in the sample of Nissen & Schuster (2010) would then only represent the ‘tip of the iceberg’ of the much larger population blue-color sequence stars studied by us and APOGEE (Hayes et al. 2018). The most natural origin of the blue-color sequence is that it is dominated by stars accreted from a satellite.

Belokurov et al. (2018) find a strong orbital anisotropy for stars with metallicities above -1.7 dex and low anisotropy for stars below this limit. They suggest that the majority of the halo stars within 30 kpc are the remnant of a massive satellite accreted during the formation of the Galactic disk between about 8 and 11 Gyr ago. The analysis of Gaia DR2 data may support this scenario for several reasons: (1) BS stars seem to constitute a significant fraction of all stars with high transverse velocities; (2) we show that they could be on a chemical evolutionary track that is less α -enriched than disk stars at the same metallicity and thus are compatible with an accreted population; (3) the kinematic properties of this BS – in particular, the high fraction of stars in retrograde orbits, a fraction of which are confined within a flattened and extended disk – and more generally the discrete wedges in the $z_{\text{max}} - R_{2\text{D,max}}$ plane – are all reminiscent of some impulsive heating of the early Galactic disk related to some accretion event(s). In this respect, the gap in the distribution of z_{max} values may mark the transition from an early phase of significant stellar accretion in the Galaxy to a more quiescent phase.

Can all stars in the blue-color sequence be attributed to a unique satellite accretion event, or is it possible that several satellites contributed to make it? From the tightness of the BS in the HRD, it is difficult to conceive that this sequence consists of populations formed in several satellite galaxies, unless their chemical and age properties at the time of their accretion were remarkably similar. Also the kinematics of stars in this sequence may be compatible with a unique – and relatively massive – merger. Fig. C.3 in Jean-Baptiste et al. (2017), for example, shows that among several satellites accreted onto a Milky Way-type galaxy, stars originating in one of them (satellite #3 in that plot) are distributed in the $E - L_z$ space in a way qualitatively similar to the BS stars we have observed, with stars having both prograde and ret-

rograde orbits, and a significant plume of stars with L_z centered around $L_z = 0$, and extending vertically to high energies. These simulations support the notion that the blue-color sequence is (at least partially) the remnant of a significant accretion event in the early history of the Milky Way. Note that Nissen & Schuster (2010); Schuster et al. (2012) have evoked the possibility that the low α stars in their work may originate from ω Cen, and at this stage we cannot reject or confirm this suggestion for the origin of the blue sequence. However, we note that ω Cen seems to have a peculiar barium abundance (Majewski et al. 2012) which appears not compatible with that of the low- α stars discussed here, see Nissen & Schuster (2011).

While our work represents only a first exploration of the stellar halo in Gaia DR2, it is clear that this mission, together with large spectroscopic surveys, is reshaping the boundaries that we had for decades assigned to the various stellar populations of the Milky Way. Our results suggest that what has been defined as the stars of the *in situ* stellar halo of the Galaxy may be in fact fossil records of its last major merger. Stars kinematically defined to belong to the inner halo comprise this possible accreted population and a sizable fraction of more metal-rich, $[\text{Fe}/\text{H}] \gtrsim -1$ dex, stars that are possibly the vestiges of the early disk of the Galaxy after it was heated by one or more merger events. But where is the parent population of the thick disk? It is possible that this progenitor, the *in situ*, chemically-defined halo is lurking in the blue sequence, but is under-represented in the volume probed by our study? So the question remains, is the *in situ* halo stellar population expected in galaxy evolution models disguised among the blue-color sequence or is it still beyond our reach?

This work has made use of data from the European Space Agency (ESA) mission Gaia (<https://www.cosmos.esa.int/gaia>), processed by the Gaia Data Processing and Analysis Consortium (DPAC, <https://www.cosmos.esa.int/web/gaia/dpac/consortium>). Funding for the DPAC has been provided by national institutions, in particular the institutions participating in the Gaia Multilateral Agreement.

REFERENCES

- Allen, C. & Santillan, A., 1991, *RMxAA*, 22, 255
 Belokurov, V., Erkal, D., Evans, N. W., Koposov, S. E., & Deason, A. J. 2018, [arXiv:1802.03414](https://arxiv.org/abs/1802.03414)
 Bonaca, A., Conroy, C., Wetzell, A., Hopkins, P. F., & Kereš, D. 2017, *ApJ*, 845, 101
 Carollo, D., Beers, T. C., Lee, Y. S., et al. 2008, *Nature*, 451, 216
 Chen, B., Stoughton, C., Smith, J. A., et al. 2001, *ApJ*, 553, 184
 Gaia Collaboration, Prusti, T., de Bruijne, J. H. J., et al. 2016, *A&A*, 595, A1
 Gaia Collaboration, Brown, A. G. A., Vallenari, A., et al. 2018a, [arXiv:1804.09365](https://arxiv.org/abs/1804.09365)
 Gaia Collaboration, Babusiaux, C., van Leeuwen, F., et al. 2018b, [arXiv:1804.09378](https://arxiv.org/abs/1804.09378)
 Gaia Collaboration, Katz, D., Antoja, T., et al. 2018c, [arXiv:1804.09380](https://arxiv.org/abs/1804.09380)
 Hayes, C. R., Majewski, S. R., Shetrone, M., et al. 2018, *ApJ*, 852, 49
 Haywood, M., Di Matteo, P., Lehnert, M., Katz, D., & Gómez, A. 2013, *A&A*, 560, A109
 Haywood, M., Di Matteo, P., Snaith, O., & Calamida, A. 2016, *A&A*, 593, A82

- Helmi, A., White, S. D. M., de Zeeuw, P. T., Zhao, H. 1999
Nature, 402, 53
- Jean-Baptiste, I., Di Matteo, P., Haywood, M., et al. 2017, A&A, 604, A106
- Koppelman, H. H., Helmi, A., & Veljanoski, J. 2018,
arXiv:1804.11347
- Lallement, R., Capitanio, L., Ruiz-Dern, L., et al. 2018,
arXiv:1804.06060
- Majewski, S. R., Nidever, D. L., Smith, V. V., et al. 2012, ApJL, 747, L37
- Malhan, K., Ibata, R. A., & Martin, N. F. 2018, arXiv:1804.11339
- Nissen, P. E., & Schuster, W. J. 2010, A&A, 511, L10
- Nissen, P. E., & Schuster, W. J. 2011, A&A, 530, A15
- Posti, L., Helmi, A., Veljanoski, J., & Breddels, M. 2017,
arXiv:1711.04766
- Pouliasis, E., Di Matteo, P., Haywood, M. 2017, A&A, 598, 66
- Reid, M. J., Menten, K. M., Brunthaler, A., et al. 2014, ApJ, 783, 130
- Schönrich, R., Binney, J., & Dehnen, W. 2010, MNRAS, 403, 1829
- Schuster, W. J., Moreno, E., Nissen, P. E., & Pichardo, B. 2012,
A&A, 538, A21
- Searle, L., & Zinn, R. 1978, ApJ, 225, 357
- Sommer-Larsen, J., & Zhen, C. 1990, MNRAS, 242, 10